Journal of Organometallic Chemistry 694 (2009) 3312–3319

Contents lists available at ScienceDirect

Journal of Organometallic Chemistry

journal homepage: www.elsevier.com/locate/jorganchem

# Reactivity of the triruthenium *ortho*-metalated cluster $[Ru_3(CO)_9\{\mu_3\text{-}\eta^1,\kappa^1,\kappa^2\text{-}PhP(C_6H_4)CH_2PPh\}]$ with tri(2-thienyl)phosphine and tri(2-furyl)phosphine: Formation of 1,3-diphenyl-2,3-dihydro-1H-1,3-benzodiphosphine complexes *via* phosphorus–carbon bond formation

Shishir Ghosh [a], Shahed Rana [a], Derek A. Tocher [b], Graeme Hogarth [b,*], Ebbe Nordlander [c,*], Shariff E. Kabir [a,*]

[a] Department of Chemistry, Jahangirnagar University, Savar, Dhaka 1342, Bangladesh
[b] Department of Chemistry, University College London, 20 Gordon Street, London WC1H OAJ, UK
[c] Inorganic Chemistry Research Group, Chemical Physics, Center for Chemistry and Chemical Engineering, Lund University, Box 124, SE-22100 Lund, Sweden

ARTICLE INFO

*Article history:*
Received 1 May 2009
Received in revised form 2 June 2009
Accepted 4 June 2009
Available online 9 June 2009

*Keywords:*
Diphosphines
Triruthenium
Carbonyl
Tri(2-thienyl)phosphine
Tri(2-furyl)phosphine
X-ray structures

ABSTRACT

Reaction of $[Ru_3(CO)_9\{\mu_3\text{-}\eta^1,\kappa^1,\kappa^2\text{-}PhP(C_6H_4)CH_2PPh\}]$ (**1**) with tri(2-thienyl)phosphine ($PTh_3$) in refluxing THF afforded $[Ru_3(CO)_9(PTh_3)(\mu\text{-dpbm})]$ (**3**) {dpbm = $PhP(C_6H_4)(CH_2)PPh$} and $[Ru_3(CO)_6(\mu\text{-}CO)_2\{\mu\text{-}\kappa^1,\eta^1\text{-}PTh_2(C_4H_2S)\}\{\mu_3\text{-}\kappa^1,\kappa^2\text{-}Ph_2PCH_2PPh\}]$ (**5**) in 18% and 12% yields, respectively, while a similar reaction with tri(2-furyl)phosphine ($PFu_3$) gave $[Ru_3(CO)_9(PFu_3)(\mu\text{-dpbm})]$ (**4**) and $[Ru_3(CO)_7(\mu\text{-}\eta^1,\eta^2\text{-}C_4H_3O)(\mu\text{-}PFu_2)\{\mu_3\text{-}\eta^1,\kappa^1,\kappa^2\text{-}PhP(C_6H_4)CH_2PPh\}]$ (**6**) in 24% and 27% yields, respectively. Compounds **2** and **4** are phosphine adducts of **1** in which the diphosphine ligand is transformed into 1,3-diphenyl-2,3-dihydro-1H-1,3-benzodiphosphine (dpbm) *via* phosphorus–carbon bond formation. Cluster **5** results from metalation of a thienyl ring, the cleaved proton being transferred to the diphosphine. Carbon–phosphorus bond cleavage of a $PFu_3$ ligand is observed in **6** to afford a phosphido-bridge and a furyl fragment, the latter bridging in a σ,π-vinyl fashion. The molecular structures of **3**, **5** and **6** have been determined by X-ray diffraction studies.



## 1. Introduction

Diphosphines are an important class of ligands that find widespread use in transition metal chemistry and homogeneous catalysis. Consequently a very wide range has been prepared, with variations to the substituents on phosphorus and the backbone group leading to the ready tuning of steric and electronic properties thus allowing highly diphosphine-dependent region- and stereoselectivity in a range of catalytic transformations. Two commonly utilized diphosphines are 1,2-bis(diphenylphosphino)benzene (dppb) [1] and bis(diphenylphosphino)methane (dppm) [2] (Chart 1), derivatives of both finding increasing use in homogeneous catalysis [3,4]. They differ primarily in the bite angles they subtend when metal-bound; the rigid *ortho*-disubstituted benzene backbone leading to a significantly increased bite angle as compared to the simple methylene group.

Like the vast majority of diphosphines studied to date, both dppm and dppb contain a single backbone unit. In contrast, diphosphines containing two linking groups are far less common and have been sparingly utilized in homogeneous catalysis although they are beginning to come under scrutiny. Notably, the coordination chemistry of diphenyl-1,4-diphospha-cyclohexane (dpdpc) [5] and 1,2,3,4-tetrahydro-1,4-diphenyl-1,4-benzodiphosphinine (bedip) [6] (Chart 1) has recently been documented. Dpdpc has been shown to act as a versatile ligand, having the ability to vary its hapticity as a function of the charge on the metal center, while complexes of both dpdpc and betip show interesting activity in the palladium-catalyzed Heck reaction of iodobenzene with styrene and ethyl acetate [5]. Both of these ligands contain a pair of two-carbon backbone groups. In contrast, in 1,3-diphenyl-2,3-dihydro-1H-1,3-benzodiphosphine (dpbm) (Chart 1) the phosphorus atoms are linked by both two- and one-atom spacers [7] which potentially increases the degree of strain in the ligand. Dpbm can be prepared upon addition of dichloromethane to $Li_2[PhP(o\text{-}C_6H_4)PPh]$, which in turn is formed from the secondary diphosphine, $PhP(H)(o\text{-}C_6H_4)P(H)Ph$ [7,8]. Uncoordinated it is proposed to exist as a mixture of *cis* and *trans* isomers, while when coordinated across a metal–metal bond only the *cis*-conformation is allowed. This isomerism relates to the stereochemistry at phosphorus, and thus once coordinated to a metal center it is diastereotopically fixed.

Dpbm can also be prepared on a metal template from relatively inexpensive dppm. Thus heating $[Ru_3(CO)_{10}(\mu\text{-dppm})]$ [9–11] in

* Corresponding authors. Tel.: +406 243 2592; fax: +406 243 2477.
*E-mail address:* skabir_ju@yahoo.com (S.E. Kabir).

0022-328X/$ - see front matter © 2009 Published by Elsevier B.V.
doi:10.1016/j.jorganchem.2009.06.005

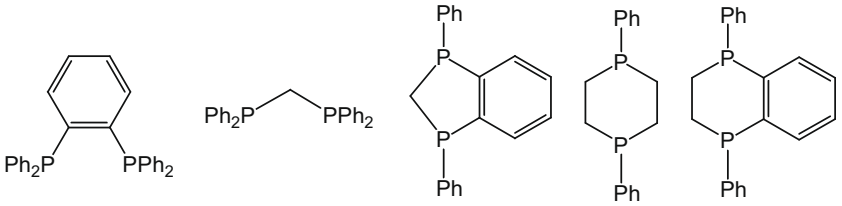


**Chart 1.**

cyclohexane for 6 h results in elimination of benzene and formation of $[Ru_3(CO)_9\{\mu_3\text{-}\eta^1,\kappa^1,\kappa^2\text{-}PhP(C_6H_4)CH_2PPh\}]$ (**1**), a transformation which is clean and high yielding. Cluster **1** has been shown to be highly reactive towards a range of unsaturated organics [12], and pertinently adds CO at elevated temperatures to afford $[Ru_3(CO)_{10}(\mu\text{-dpbm})]$ (**2**) in high yields [9,10], a transformation which can be reversed upon heating (Scheme 1).

This seemed to us a useful way of preparing a range of dpbm complexes in a number of simple and high yielding steps. A limitation of **2** is its ready loss of CO and regeneration of **1** *via* carbon–phosphorus bond cleavage. We reasoned that the addition of a tertiary phosphine to **1** would potentially lead to phosphine-substituted derivatives that were less prone to ligand loss and hence cleavage of the dpbm ligand. With this in mind and as part of our study on the reactivity of functionalized phosphines with transition metal carbonyls, we have examined the reactivity of tri(2-thienyl)phosphine ($PTh_3$) and tri(2-furyl)phosphine ($PFu_3$) with **1**, the results of which are described herein.

## 2. Experimental

Unless otherwise stated all the reactions were performed under a nitrogen atmosphere using standard Schlenk techniques. Solvents were dried and distilled prior to use by standard methods. $[Ru_3(CO)_{12}]$ was purchased from Strem Chemicals Inc. and used without further purification and $[Ru_3(CO)_9\{\mu_3\text{-}\eta^1,\kappa^1,\kappa^2\text{-}PhP(C_6H_4)CH_2PPh\}]$ (**1**) was prepared according to the published procedures [11]. Bis(diphenylphosphino)methane (dppm), $PFu_3$ and $PTh_3$ were purchased from Merck and used as received. All reactions were carried out under a nitrogen atmosphere using standard Schlenk techniques. Reagent-grade solvents were dried by standard methods prior to use. Infrared spectra were recorded on a Shimadzu FTIR 8101 spectrophotometer. $^1$H NMR spectra were recorded on a Bruker DPX 400 spectrometer. Elemental analyses were performed by Microanalytical Laboratories, University College London.

### 2.1. Reaction of *1* with $PTh_3$

To a THF solution (20 mL) of **1** (100 mg, 0.116 mmol) was added $PTh_3$ (32 mg, 0.114 mmol) and the reaction mixture was heated to reflux for 90 min. The solvent was removed by rotary evaporation and the residue chromatographed by TLC on silica gel. Elution with hexane/$CH_2Cl_2$ (7:3, v/v) developed three bands. The first band was unreacted **1** (trace). The second band afforded $[Ru_3(CO)_6(\mu\text{-}CO)_2\{\mu\text{-}\kappa^1,\eta^1\text{-}PTh_2(C_4H_2S)\}\{\mu_3\text{-}\kappa^1,\kappa^2\text{-}Ph_2PCH_2PPh\}]$ (**5**) (16 mg, 12%) as orange crystals while the third band gave $[Ru_3(CO)_9(PTh_3)(\mu\text{-dpbm})]$ (**3**) (23 mg, 18%) as red crystals after recrystallization from hexane/$CH_2Cl_2$ at 4 °C. Spectral data for **3**: *Anal.* Calc. for $C_{40}H_{25}O_9P_3Ru_3S_3$: C, 42.07; H, 2.21. Found: C, 42.44; H, 2.28%. IR ($\nu$CO, $CH_2Cl_2$): 2058 m, 1998 s, 1978 s, 1942 s cm$^{-1}$; $^1$H NMR ($CDCl_3$): $\delta$ 7.81(m, 4H), 7.55(m, 9H), 7.38 (m, 3H), 7.30 (m, 4H), 7.12 (m, 3H), 4.24 (m, 1H), 3.57 (m, 1H); $^{31}$P{$^1$H} NMR ($CDCl_3$): $\delta$ 29.9 (s, 2P), −1.5 (s, 1P). Spectral data for **5**: *Anal.* Calc. for $C_{39}H_{25}O_8P_3Ru_3S_3$: C, 42.05; H, 2.26. Found: C, 42.41; H, 2.32%. IR ($\nu$CO, $CH_2Cl_2$): 2040 w, 2027 w, 1990 m, 1968 s, 1943sh cm$^{-1}$; $^1$H NMR ($CDCl_3$): $\delta$ 7.75 (m, 5H), 7.60 (m, 5H), 7.51–7.21 (m, 6H), 7.20 (m, 4H), 7.16 (m, 1H), 7.09 (m, 1H), 6.90 (m, 1H), 3.81(m, 1H), 3.55 (m, 1H).

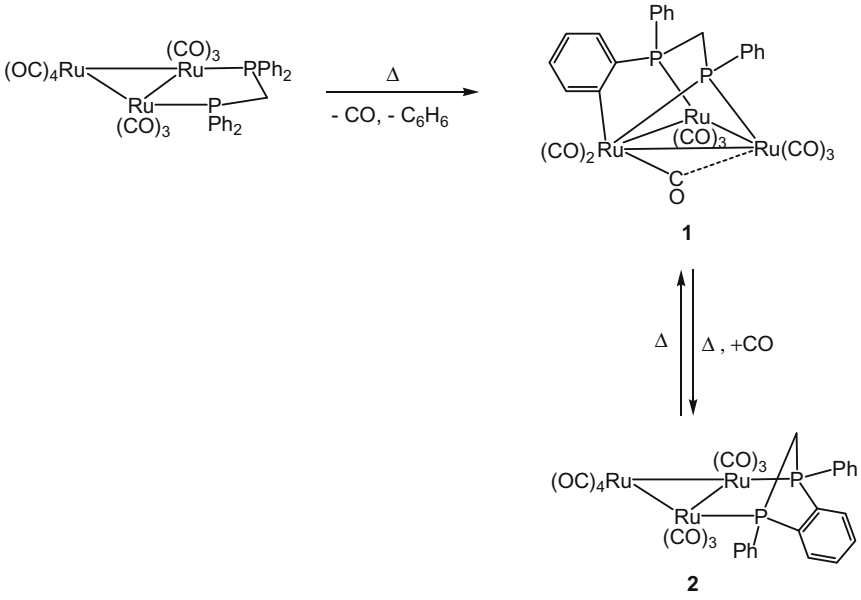


**Scheme 1.**

$^{31}P\{^1H\}$ NMR ($CDCl_3$): $\delta$ 33.3 (d, 1P, $J$ = 72.6 Hz), 29.1 (d, 1P, $J$ = 72.6 Hz), −4.2 (s, 1P).

### 2.2. Reaction of **1** with $PFu_3$

A similar reaction to that above between **1** (100 mg, 0.116 mmol) and $PFu_3$ (27 mg, 0.116 mmol) in refluxing THF (20 mL) followed by similar chromatographic separation developed three bands. The first band was unreacted **1** (trace). The second band gave $[Ru_3(CO)_9(PFu_3)(\mu\text{-dpbm})]$ (**4**) (30 mg, 24%) as red crystals while the third band afforded $[Ru_3(CO)_7(\mu\text{-}\eta^1,\eta^2\text{-}C_4H_3O)(\mu\text{-}PFu_2)\{\mu_3\text{-}\eta^1,\kappa^1,\kappa^2\text{-}PhP(C_6H_4)CH_2PPh\}]$ (**6**) (33 mg, 27%) as orange crystals from hexane/$CH_2Cl_2$ at 4 °C. Spectral data for **4**: *Anal.* Calc. for $C_{40}H_{25}O_{12}P_3Ru_3$: C, 43.93; H, 2.31. Found: C, 44.27; H, 2.39%. IR ($\nu$CO, $CH_2Cl_2$): 2071 w, 2045 m, 2002 s, 1985 s, 1953 m $cm^{-1}$; $^1H$ NMR ($CDCl_3$): $\delta$ 7.96 (m, 1H), 7.82 (m, 2H), 7.57 (m, 5H), 7.22 (m, 1H), 6.99 (m, 2H), 6.88 (m, 2H), 6.70 (m, 2H), 6.33 (m, 4H), 6.26 (m, 2H), 6.20 (m, 2H), 4.27 (m, 1H), 3.51 (m, 1H); $^{31}P\{^1H\}$ NMR ($CDCl_3$): $\delta$ 4.5 (d, 1P, $J$ = 77.2 Hz), −0.5 (d, 1P, $J$ = 77.2 Hz), −17.9 (s, 1P); mass spectrum (FAB): $m/z$ 1093 ($M^+$). Spectral data for **6**: *Anal.* Calc. for $C_{38}H_{25}O_{10}P_3Ru_3$: C, 43.98; H, 2.43. Found: C, 44.34; H, 2.51%. IR ($\nu$CO, $CH_2Cl_2$): 2072 s, 2038 m, 2012 s, 1954 m, br $cm^{-1}$; $^1H$ NMR ($CDCl_3$): $\delta$ 8.27(m, 1H), 7.85(m, 1H), 7.64 (m, 3H), 7.53 (m, 1H), 7.46 (m, 3H), 7.35 (m, 4H), 7.14 (m, 1H), 6.98 (m, 1H), 6.79 (m, 1H), 6.64 (m, 1H), 6.31 (m, 2H), 6.21 (m, 1H), 6.14 (m, 2H), 6.01 (m, 1H), 2.32 (m, 1H), 1.96 (m, 1H); $^{31}P\{^1H\}$ NMR ($CDCl_3$): $\delta$ 68.3 (d, 1P, $J$ = 30.7 Hz,), 67.0 (d, 1P, $J$ = 81.6 Hz), 0.5 (dd, 1P, $J$ = 81.6, 30.7 Hz).

### 2.3. X-ray structure determinations

Single crystals of **3**, **5** and **6** suitable for X-ray diffraction were grown by slow diffusion of hexane into a dichloromethane solution at 4 °C. All geometric and crystallographic data were collected at 150 K (for **3** and **5**) and 293 K (for **6**) on a Bruker SMART APEX CCD diffractometer using Mo K$\alpha$ radiation ($\lambda$ = 0.71073 Å). Data reduction and integration were carried out with SAINT+ and absorption corrections were applied using the program SADABS [13]. Structures were solved by direct methods and developed using alternating cycles of least-squares refinement and difference-Fourier synthesis. All non-hydrogen atoms were refined anisotropically. Hydrogen atoms were placed in the calculated positions and their thermal parameters linked to those of the atoms to which they were attached (riding model). The SHELXTL PLUS V6.10 program package was used for structure solution and refinement [14]. Final difference maps did not show any residual electron density of stereochemical significance. The details of the data collection and structure refinement are given in Table 1.

## 3. Results

### 3.1. Synthesis and characterization of dpbm complexes $[Ru_3(CO)_9\{P(C_4H_3E)_3\}(\mu\text{-dpbm})]$ (E = S, O)

Reaction of $[Ru_3(CO)_9\{\mu_3\text{-}\eta^1,\kappa^1,\kappa^2\text{-}PhP(C_6H_4)CH_2PPh\}]$ (**1**) with $PTh_3$ and $PFu_3$ in refluxing THF leads to the isolation of the desired dpbm complexes $[Ru_3(CO)_9(PTh_3)(\mu\text{-dpbm})]$ (**3**) and $[Ru_3(CO)_9(PFu_3)(\mu\text{-dpbm})]$ (**4**) in moderate (18% and 24%) yields (Scheme 2).

Formation of dpbm complexes was shown spectroscopically with $^{31}P\{^1H\}$ NMR spectra being particularly informative. For **3** this consists of two singlets at $\delta$ 29.9 and −1.5 ppm in a 2:1 ratio being attributed to the dpbm and $PTh_3$ ligands, respectively. The former is consistent with the observation of a singlet for **2** at $\delta$ 28.8 ppm [9]. The equivalence of the two ends of the dpbm ligand suggests that in solution the monodentate phosphine is moving rapidly between the two equatorial sites (Scheme 3), an observation which is fully consistent with the observed fluxional behavior of related $[Ru_3(CO)_9(PR_3)(\mu\text{-dppm})]$ complexes [15]. In contrast, the $^{31}P\{^1H\}$ NMR spectrum of **4** consists of a pair of doublets at $\delta$ 4.5 and −0.5 ppm ($J_{PP}$ = 77.2 Hz) assigned to the dpbm ligand and a singlet at $\delta$ −17.9 ppm attributed to the $PFu_3$ ligand. This suggests that in **4** movement of the $PFu_3$ ligand is slow on the NMR timescale.

In the aliphatic region of the $^1H$ NMR spectrum, both display two complex equal intensity multiplets being assigned to the

**Table 1**
Crystallographic data and structure refinement for **3**, **5** and **6**.

| | **3** | **5** | **6** |
|---|---|---|---|
| Empirical formula | $C_{40}H_{25}O_9P_3Ru_3S_3$ | $C_{42}H_{39}O_8P_3Ru_3S_3$ | $C_{44}H_{24}O_{10}P_3Ru_3$ |
| Formula weight (Å) | 1141.90 | 1164.03 | 1108.75 |
| Temperature (K) | 150(2) | 150(2) | 293(2) |
| Crystal system | Triclinic | Monoclinic | Triclinic |
| Space group | $P\bar{1}$ | $P2_1/c$ | $P\bar{1}$ |
| Unit cell dimensions | | | |
| $a$ (Å) | 10.3086(7) | 11.2555(10) | 11.6443(11) |
| $b$ (Å) | 13.6048(10) | 19.8514(17) | 12.0494(11) |
| $c$ (Å) | 16.2662(12) | 18.6841(16) | 15.0970(14) |
| $\alpha$ (°) | 105.816(1) | 90 | 98.961(2) |
| $\beta$ (°) | 107.012(1) | 95.078(2) | 98.381(1) |
| $\gamma$ (°) | 92.232(1) | 90 | 100.374(2) |
| Volume (Å$^3$) | 2081.3(3) | 4158.3(6) | 2025.0(3) |
| $Z$ | 2 | 4 | 2 |
| Density (calculated) (Mg/m$^3$) | 1.822 | 1.859 | 1.818 |
| Absorption coefficient (mm$^{-1}$) | 1.395 | 1.396 | 1.284 |
| F(0 0 0) | 1124 | 2320 | 1090 |
| Crystal size (mm) | 0.22 × 0.18 × 0.06 | 0.12 × 0.04 × 0.01 | 0.42 × 0.22 × 0.18 |
| $\theta$ Range for data collection (°) | 2.44–28.27 | 1.50–28.25 | 1.75–28.30 |
| Reflections collected ($R_{int}$) | 18 007 | 35 854 | 17 526 |
| Independent reflections | 9494 (0.0218) | 9924 (0.0722) | 9236 (0.0233) |
| Data/restraints/parameters | 9494/0/523 | 9924/0/521 | 9236/10/682 |
| Goodness-of-fit on $F^2$ | 1.004 | 1.000 | 0.992 |
| Final $R$ indices [$I > 2\sigma(I)$] | $R_1$ = 0.0343, $wR_2$ = 0.0981 | $R_1$ = 0.0537, $wR_2$ = 0.1155 | $R_1$ = 0.0501, $wR_2$ = 0.1436 |
| $R$ indices (all data) | $R_1$ = 0.0395, $wR_2$ = 0.1018 | $R_1$ = 0.0811, $wR_2$ = 0.1268 | $R_1$ = 0.0557, $wR_2$ = 0.1500 |
| Largest difference in peak and hole (e Å$^{-3}$) | 1.135 and −1.233 | 2.291 and −0.950 | 1.243 and −2.429 |

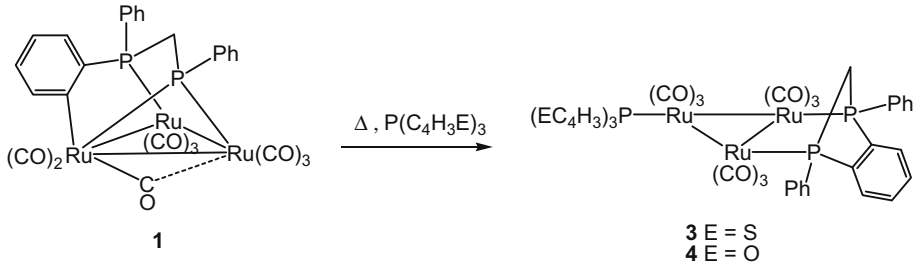


**Scheme 2.**

inequivalent methylene protons of the backbone. For **3** these appear at $\delta$ 4.24 and 3.57 and for **4** at $\delta$ 4.27 and 3.51. Both also show parent molecular ions in their FAB mass spectra together with ions due to sequential loss of all nine carbonyl ligands.

Cluster **3** was also characterized by single crystal X-ray crystallography. An ORTEP diagram of the molecular structure is depicted in Fig. 1, and selected bond distances and angles are listed in the caption. The molecule comprises a triangle of ruthenium atoms with three distinctly different ruthenium–ruthenium bonds; [Ru(1)–Ru(2) 2.8585(4), Ru(1)–Ru(3) 2.8351(4) and Ru(2)–Ru(3) 2.8868(3) Å]. The $PTh_3$ ligand occupies an equatorial coordination site on the remote metal, Ru(1), while the dpbm ligand bridges the Ru(2)–Ru(3) edge and also lies in the equatorial plane. These features are fully consistent with the observed structures of $[Ru_3(CO)_9(PR_3)(\mu\text{-dppm})]$ [12,15–16]. The Ru–P bond distances involving the dpbm ligand [Ru(2)–P(2) 2.3197(8) and Ru(3)–P(3) 2.3131(8) Å] are very similar to those observed in both polymorphs of $[Ru_3(CO)_{10}(\mu\text{-dpbm})]$ [av. Ru–P 2.3215(1) Å] [9,17].

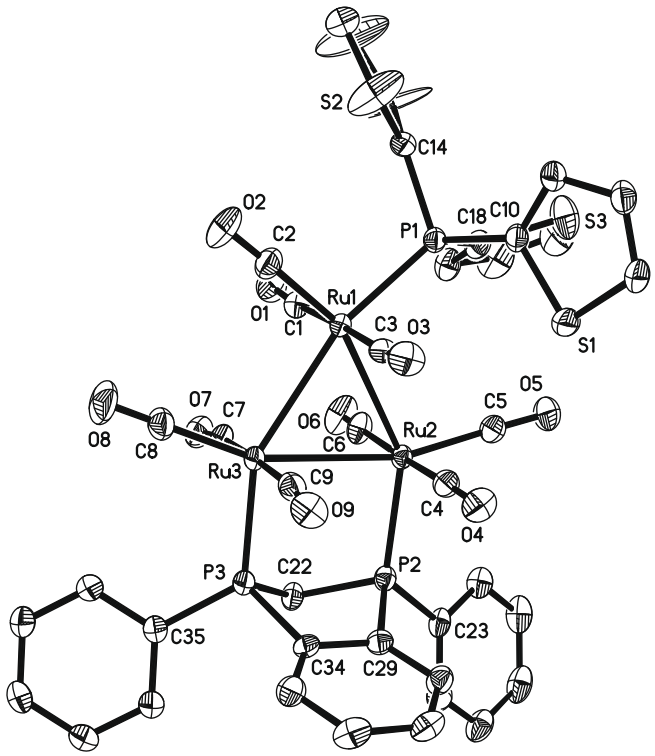


**Fig. 1.** Molecular structure of $[Ru_3(CO)_9(PTh_3)(\mu\text{-dpbm})]$ (**3**) showing 50% probability thermal ellipsoids. Hydrogen atoms are omitted for clarity. Selected bond lengths (Å) and angles (°): Ru(1)–Ru(2) 2.8585(4), Ru(1)–Ru(3) 2.8351(4), Ru(2)–Ru(3) 2.8868(3), Ru(1)–P(1) 2.3261(8), Ru(2)–P(2) 2.3197(8), Ru(3)–P(3) 2.3131(8), Ru(3)–Ru(1)–Ru(2) 60.930(8), Ru(1)–Ru(2)–Ru(3) 59.135(9), Ru(1)–Ru(3)–Ru(2) 59.935(9), C(1)–Ru(1)–C(3) 176.52(13), C(2)–Ru(1)–P(1) 101.21(11), C(3)–Ru(1)–P(1) 92.34(9), P(1)–Ru(1)–Ru(2) 101.90(2), P(1)–Ru(1)–Ru(3) 162.74(2), P(2)–Ru(2)–Ru(3) 87.40(2), C(5)–Ru(2)–P(2) 108.40(10), P(3)–Ru(3)–Ru(2) 90.22(2), C(8)–Ru(3)–P(3) 109.17(11), C(22)–P(3)–Ru(3) 109.53(11), C(34)–P(3)–C(22) 92.56(14), C(35)–P(3)–C(22) 106.87(14), C(35)–P(3)–Ru(3) 122.66(11), P(2)–C(22)–P(3) 98.96(15).

### 3.2. Carbon-element bond cleavage products

In both reactions a second product was isolated (Scheme 4). With $PTh_3$ this was found to be $[Ru_3(CO)_6(\mu\text{-}CO)_2\{\mu\text{-}\kappa^1,\eta^1\text{-}PTh_2(C_4H_2S)\}\{\mu_3\text{-}\kappa^1,\kappa^2\text{-}Ph_2PCH_2PPh\}]$ (**5**) (12%), which results from *ortho*-metalation of a thienyl ring with transfer of the proton to the *ortho*-metalated arene ring of **1**. With $PFu_3$ the dominant side-reaction was the carbon–phosphorus bond scission of a furyl group leading to the isolation of $[Ru_3(CO)_7(\mu\text{-}\eta^1,\eta^2\text{-}C_4H_3O)(\mu\text{-}PFu_2)\{\mu_3\text{-}\eta^1,\kappa^1,\kappa^2\text{-}PhP(C_6H_4)CH_2PPh\}]$ (**6**) in 27% yield. Both **5** and **6** are formed only in very low yields at room temperature, and it was found that their yields increase relative to that of dpbm complexes **3** and **4** when the reaction between **1** and $PFu_3$ was carried in refluxing benzene. Both **5** and **6** were characterized by single crystal X-ray crystallography.

An ORTEP diagram of the molecular structure of **5** is depicted in Fig. 2, and the caption contains selected bond distances and angles. The cluster consists of an approximate isosceles triangle of ruthenium atoms [Ru(1)–Ru(2) 2.8468(6), Ru(1)–Ru(3) 2.8857(6) and Ru(2)–Ru(3) 2.8908(6) Å] coordinated by six terminal CO and two semi-bridging CO ligands, a $\mu\text{-}Th_2PC_4H_2S$ ligand and a $\mu_3\text{-}Ph_2PCH_2PPh$ ligand. The semi-bridging carbonyls span Ru(1)–Ru(3) and Ru(2)–Ru(3), their asymmetric nature being apparent from the corresponding ruthenium–carbon distances [Ru(1)–C(8) 2.445(5), Ru(3)–C(8) 1.995(5), Ru(2)–C(7) 2.575(5) and Ru(3)–C(7) 1.945(6) Å]. The $\mu\text{-}Th_2PC_4H_2S$ ligand bridges the Ru(1)–Ru(3) edge such that the phosphorus atom is bound to Ru(1) and the *ortho*-metalated thienyl ring to Ru(3). The Ru(3)–C(52) distance of 2.128(5) Å is similar to those observed in related complexes such as $[Ru_3(CO)_9(\mu\text{-}H)\{\mu_3\text{-}\kappa^1,\eta^1,\eta^2\text{-}Ph_2P(C_4H_2S)\}]$ (2.10(1) Å) and $[Ru_3(CO)_8(PPh_2Th)(\mu\text{-}H)\{\mu_3\text{-}\kappa^1,\eta^1,\eta^2\text{-}Ph_2P(C_4H_2S)\}]$ (2.114(4) Å) [18]. As far as we are aware, **5** is the first ruthenium complex in which the $PTh_3$ ligand adopts this type of $(\mu\text{-}\kappa^1,\eta^1)$ coordination mode. However, this mode of coordination of $PTh_3$ ligand has been previously observed in the triosmium cluster $[Os_3(CO)_9(\mu\text{-}H)\{\mu\text{-}\kappa^1,\eta^1\text{-}PTh_2(C_4H_2S)\}]$ [19]. The $\mu_3\text{-}Ph_2PCH_2PPh$ ligand is facially located on the opposite side of the triruthenium core, such that one phosphorus is bound to Ru(3) while the other bridges the Ru(1)–Ru(3) edge. The coordination mode of this fragment is similar to that observed in $[Ru_3(CO)_9(\mu\text{-}H)\{\mu_3\text{-}\kappa^1,\kappa^2\text{-}Ph_2PCH_2PPh\}]$ [9]. Spectroscopic data for **5** are consistent with the solid-state structure. In addition to the aromatic proton resonances for the diphosphine and thienyl phosphine ligands, the $^1H$ NMR spectrum exhibits two multiplets at $\delta$ 3.81 and 3.55, each integrating to 1H, being attributed to the methylene proton of the diphosphine ligand. The $^{31}P\{^1H\}$ NMR spectrum consists of a pair of doublets ($J$ = 72.6 Hz) at 33.3 and 29.1 ppm assigned to the diphosphine and a further singlet at −4.2 ppm attributed to the *ortho*-metalated trithienylphosphine.

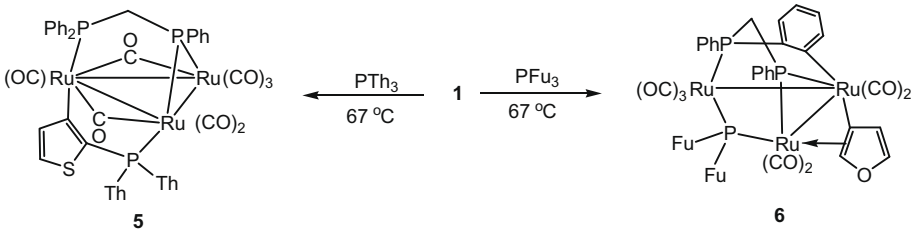


**Scheme 4.**

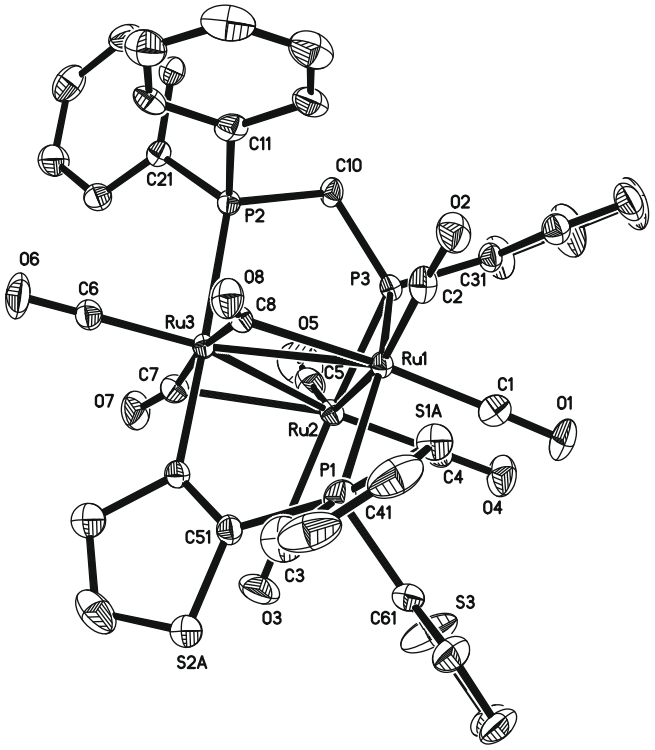


**Fig. 2.** Molecular structure of $[Ru_3(CO)_6(\mu\text{-}CO)_2\{\mu\text{-}\kappa^1,\eta^1\text{-}PTh_2(C_4H_2S)\}\{\mu_3\text{-}\kappa^1,\kappa^2\text{-}Ph_2PCH_2PPh\}]$ (**5**) showing 50% probability thermal ellipsoids. Hydrogen atoms are omitted for clarity. Selected bond lengths (Å) and angles (°): Ru(1)–Ru(2) 2.8468(6), Ru(1)–Ru(3) 2.8857(6), Ru(2)–Ru(3) 2.8908(6), Ru(1)–P(1) 2.3668(14), Ru(1)–P(3) 2.3115(14), Ru(2)–P(3) 2.3168(14), Ru(3)–P(2) 2.3841(14), Ru(3)–C(52) 2.128(5), Ru(1)–C(8) 2.445(5), Ru(3)–C(8) 1.995(5), Ru(2)–C(7) 2.575(5), Ru(3)–C(7) 1.945(6), Ru(2)–Ru(1)–Ru(3) 60.562(14), Ru(1)–Ru(2)–Ru(3) 60.384(15), Ru(1)–Ru(3)–Ru(2) 59.054(14), P(3)–Ru(1)?Ru(2) 52.13(3), P(1)–Ru(1)–Ru(3) 87.84(3), P(3)–Ru(2)–Ru(1) 51.96(3), C(52)–Ru(3)–P(2) 174.76(14), P(2)–Ru(3)–Ru(1) 91.41(3), C(52)–Ru(3)–Ru(2) 90.10(13), Ru(1)–P(3)–Ru(2) 75.92(4), Ru(3)–C(8)–Ru(1) 80.37(18), Ru(3)–C(7)–Ru(2) 78.15(18), O(8)–C(8)–Ru(3) 153.9(4), O(8)–C(8)–Ru(1) 125.6(4), O(7)–C(7)–Ru(3) 159.5(5), O(7)–C(7)–Ru(2) 121.8(4), P(2)–C(10)–P(3) 105.7(3).

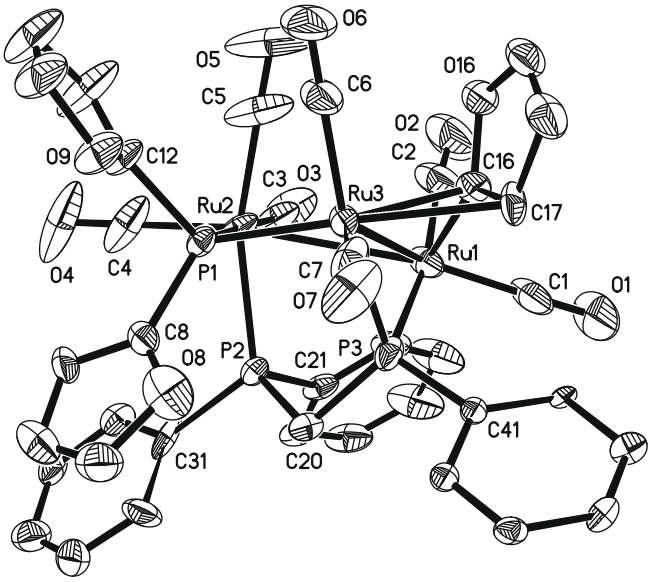


**Fig. 3.** Molecular structure of $[Ru_3(CO)_7(\mu\text{-}\eta^1,\eta^2\text{-}C_4H_3O)(\mu\text{-}PFu_2)\{\mu_3\text{-}\eta^1,\kappa^1,\kappa^2\text{-}PhP(C_6H_4)CH_2PPh\}]$ (**6**) showing 50% probability thermal ellipsoids. Hydrogen atoms are omitted for clarity. Selected bond lengths (Å) and angles (°): Ru(1)–Ru(2) 3.1181(6), Ru(1)–Ru(3) 3.0914(6), Ru(2)–P(1) 2.3505(11), Ru(3)–P(1) 2.2400(11), Ru(2)–P(2) 2.3795(11), Ru(1)–P(3) 2.3491(14), Ru(3)?P(3) 2.3673(12), Ru(1)–C(16) 2.259(14), Ru(1)–C(22) 2.175(5), Ru(3)–C(16) 2.265(11), Ru(3)–C(17) 2.569(11), Ru(3)–Ru(1)–Ru(2) 61.456(12), P(3)–Ru(1)–Ru(3) 49.30(3), P(3)–Ru(1)–Ru(2) 80.10(3), P(1)–Ru(2)–P(2) 90.13(4), P(1)–Ru(2)–Ru(1) 101.00(3), P(2)–Ru(2)–Ru(1) 73.64(3), P(1)–Ru(3)–P(3) 95.87(4), P(1)–Ru(3)–Ru(1) 104.51(3), P(3)–Ru(3)–Ru(1) 48.79(3), Ru(3)–P(1)–Ru(2) 87.42(4), Ru(1)–P(3)–Ru(3) 81.91(4), P(2)–C(20)–P(3) 105.7(2), C(22)–Ru(1)?C(16) 170.5(5), C(2)–Ru(1)–C(22) 91.0(2), C(22)–Ru(1)–Ru(3) 130.65(13).

An ORTEP diagram of the molecular structure of **6** is shown in Fig. 3, and selected bond distances and angles are listed in the caption. The molecule contains an open triangle of ruthenium atoms capped by a $\mu_3$-$PhP(C_6H_4)CH_2PPh$ ligand and bridging di(2-furyl)phosphide and furyl groups. The diphosphine bridges all ruthenium atoms in a similar fashion to that observed in **1**; that is Ru(2) is bonded to one phosphorus atom while the other is bonded to Ru(3) and this phosphorus atom together with the C(22) carbon of the $C_6H_4$ moiety are bonded to Ru(1). The Ru–C [2.175(5) Å] and average Ru–P [av. 2.3653(12) Å] distances are also similar to those in **1**. The open edge of the metal triangle is asymmetrically bridged by a di(2-furyl)phosphide ligand, bond angles and distances being similar to those found in other open triruthenium clusters in which the open edge is bridged by a phosphido ligand [20,21]. The furyl bridge spans across the Ru(1)–Ru(3) edge in a σ,π-vinyl fashion being bound to Ru(1) via a σ-bond. The Ru(1)–Ru(2) edge [3.1181(6) Å], bridged by the $PhPC_6H_4$ moiety of the diphosphine, is longer than the Ru(1)–Ru(3) edge [3.0914(6) Å] which is simultaneously bridged by furyl and phosphido bridges. Spectroscopic data are consistent with the solid-state structure. The $^1$H NMR spectrum shows multiplets at $\delta$ 2.32 and 1.96 assigned to the methylene proton of the diphosphine and the $^{31}P\{^1H\}$ NMR spectrum shows two doublets of doublets at $\delta$ 68.3 and 67.0 ppm and a further doublet at $\delta$ 0.5 ppm, each integrating to one phosphorus.

## 4. Discussion

Few reactivity studies have been carried out directly on $[Ru_3(CO)_9\{\mu_3\text{-}\eta^1,\kappa^1,\kappa^2\text{-}PhP(C_6H_4)CH_2PPh\}]$ (**1**) [9,10] although it has been implicated in thermal reactions of $[Ru_3(CO)_{10}(\mu\text{-dppm})]$ [12]. Bonnet and co-workers [9] have shown that formation of **2** upon carbonylation of **1** proceeds *via* the initial addition of CO to the cluster with concomitant ruthenium–ruthenium bond cleavage

to afford $[Ru_3(CO)_{10}\{\mu_3\text{-}\eta^1,\kappa^1,\kappa^2\text{-}PhP(C_6H_4)CH_2PPh\}]$ (**7**) which has been crystallographically characterized (Scheme 5). Likewise, addition of $PPh_3$ at 0 °C has been shown to initially afford **8** resulting from phosphine addition and ruthenium–ruthenium bond scission [10]. Addition of further phosphine and warming to room temperature result in further metal–metal bond scission to afford binuclear **9** and mononuclear $[Ru(CO)_3(PPh_3)_2]$ [22]. In previous work we have characterized cluster **10** (Scheme 5) which results from addition of two equivalents of phosphine [21]. Here both phosphorus–hydrogen bonds have been activated leading to the formation of a hydride and transfer of a second proton to the *ortho*-metalated ring. Unfortunately, we carried out this reaction at elevated temperature (80 °C) and we were therefore unable to identify any intermediates. Nevertheless it seems likely that the reaction proceeds in an analogous fashion to that with $PPh_3$, initial addition leading to ruthenium–ruthenium bond scission followed by later addition of the phosphorus–hydrogen bonds. Given that we did not isolate $[Ru(CO)_3(Ph_2PH)_2]$ [23] from this reaction we believe that the first phosphorus–hydrogen additions occur *prior* to addition of the second equivalent of phosphine.

On the basis of the chemistry discussed above we propose a plausible mechanism for the formation of clusters **3**–**6** (Scheme 6). Initial phosphine addition is expected to afford open 50-electron clusters $[Ru_3(CO)_9\{P(C_4H_3E)_3\}\{\mu_3\text{-}\eta^1,\kappa^1,\kappa^2\text{-}PhP(C_6H_4)CH_2PPh\}]$ (**A**). These can then rearrange *via* carbon–phosphorus and ruthenium–ruthenium bond formation to give the isomeric dpbm complexes **3** and **4** which we isolated in moderate yields. We have not been able to ascertain whether this transformation is reversible. Competing pathways to the thermal rearrangement of **A** presumably exist. For $PTh_3$ this apparently involves carbonyl loss and *ortho*-metalation of one of the thienyl groups, possibly proceeding *via* a bridging hydride intermediate (shown), followed by transfer of this proton to the *ortho*-metalated arene ring of the diphosphine ligand to afford the observed product **5**. In contrast, for $PFu_3$ the competing process is carbon–phosphorus bond scission together with loss of two carbonyls leading to the generation of **6** which contains phosphido and furyl bridges.

Aspects of our recent work on a comparative study of the reactivity of $[Ru_3(CO)_{10}(\mu\text{-dppm})]$ with $PTh_3$ and $PFu_3$ shed some light on these secondary processes. Thus, while in each case the simple substitution products, $[Ru_3(CO)_9\{P(C_4H_3E)_3\}(\mu\text{-dppm})]$, are initially formed, upon mild heating they undergo both carbon–phosphorus and carbon–hydrogen bond cleavage to afford thiophyne and furyne clusters $[Ru_3(CO)_7(\mu\text{-dppm})(\mu_3\text{-}\eta^2\text{-}C_4H_2E)\{\mu\text{-}P(C_4H_3E)_2\}(\mu\text{-}H)]$ (Scheme 7) [20]. This provides evidence for both the facile carbon–hydrogen and carbon–phosphorus activation of the coordinated ligands.

In the work described herein the coordinated $PTh_3$ and $PFu_3$ ligands undergo different thermal activation pathways. Again, this is not surprising in light of the established sensitivity of phosphorus–carbon bond cleavage reactions to changes in the substituents on carbon [24]. In recent work focused on their thermal rearrangement when bound to dirhenium and dimanganese centers such behavior has been noted, with $PTh_3$ generally showing a greater propensity to undergo carbon–phosphorus bond cleavage than $PFu_3$ [25,26]. It is noteworthy that when these ligands are bound to the triruthenium framework this trend appears to be reversed. Another explanation is that in each case both carbon–hydrogen and carbon–phosphorus bond activation occurs and the selectivity we observe in product isolation simply reflects the thermodynamic stability of the products generated from these two different transformations.

## 5. Conclusions

In summary, the reaction of **1** with $PTh_3$ and $PFu_3$ at 68 °C leads to the desired 1,3-diphenyl-2,3-dihydro-1H-1,3-benzodiphosphine (dpbm) compounds $[Ru_3(CO)_9(PTh_3)(\mu\text{-dpbm})]$ (**3**) and $[Ru_3(CO)_9(PFu_3)(\mu\text{-dpbm})]$ (**4**), formed as a result of phosphorus–carbon bond formation, albeit in moderate yields. The latter may be due to competing transformations of the non-innocent added phosphines since secondary products are $[Ru_3(CO)_6(\mu\text{-}CO)_2\{\mu\text{-}\kappa^1,\eta^1\text{-}PTh_2(C_4H_2S)\}\{\mu_3\text{-}\kappa^1,\kappa^2\text{-}Ph_2PCH_2PPh\}]$ (**5**), resulting from carbon–hydrogen migration from the monodentate to bidentate phos-

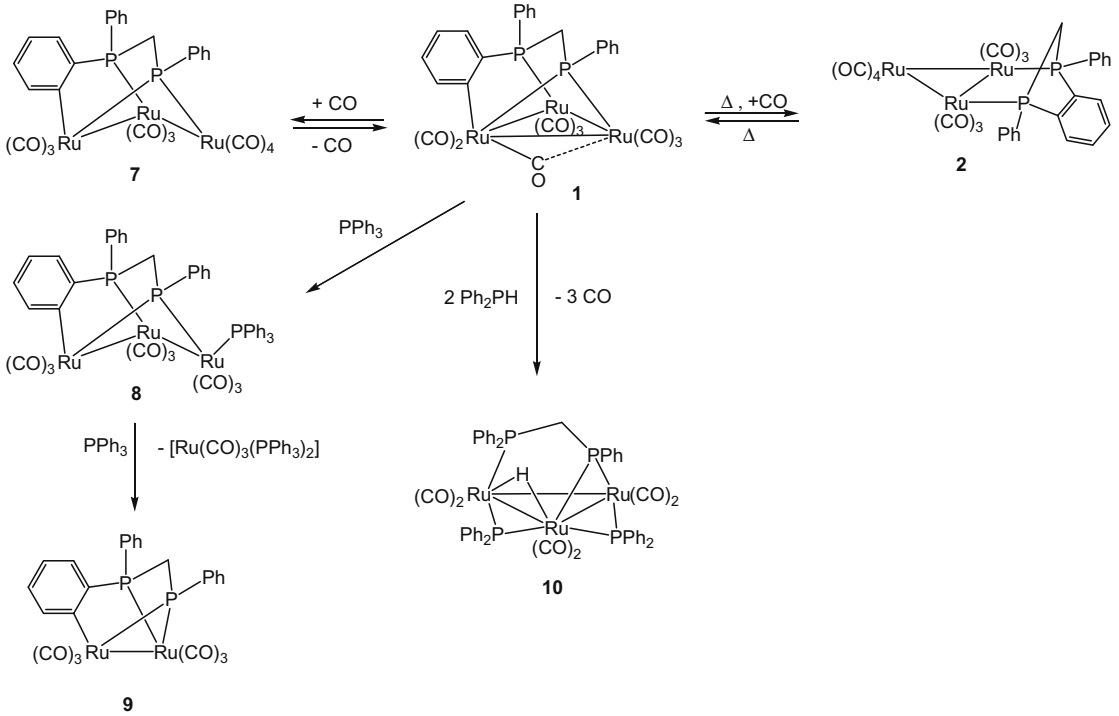


**Scheme 5.**

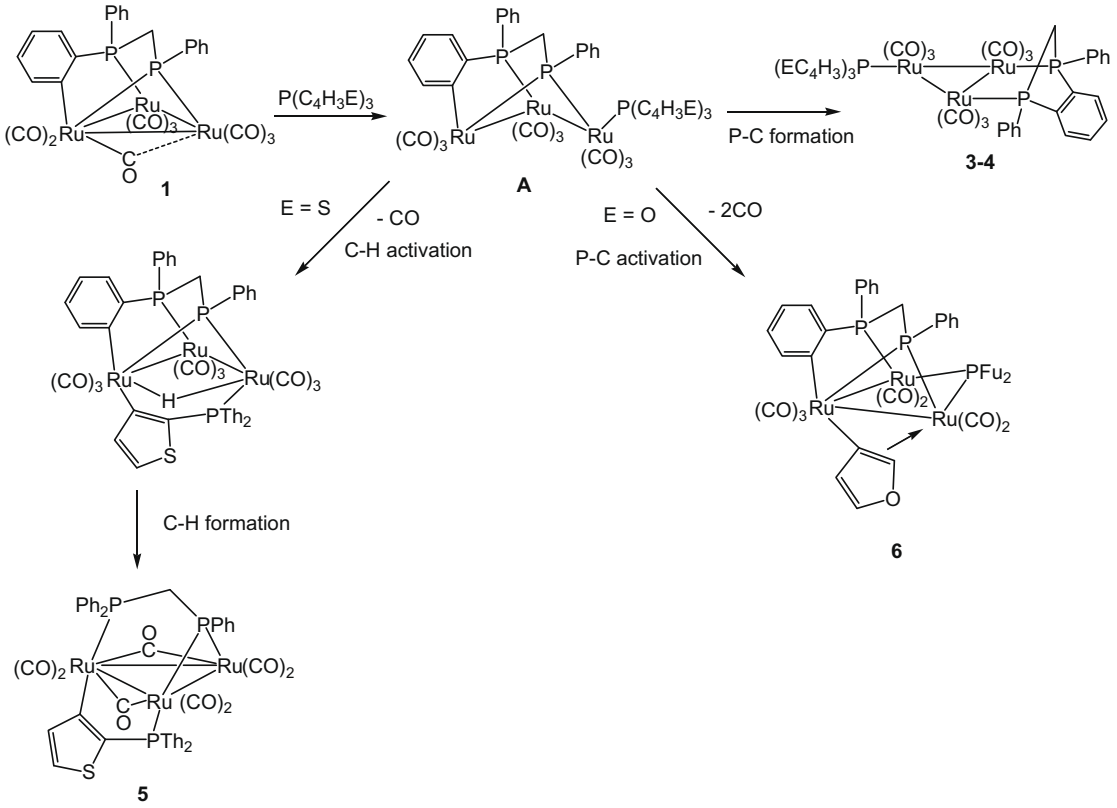


Scheme 6.

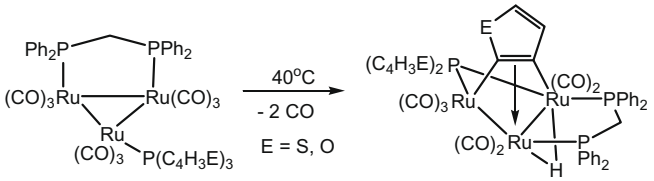


Scheme 7.

phine, and $[Ru_3(CO)_7(\mu\text{-}\eta^1,\eta^2\text{-}C_4H_3O)(\mu\text{-}PFu_2)\{\mu_3\text{-}\eta^1,\kappa^1,\kappa^2\text{-}PhP(C_6H_4)CH_2PPh\}]$ (**6**) formed *via* carbon–phosphorus bond cleavage. In an attempt to cleave a carbon–phosphorus bond of the $PTh_3$ ligand, we also conducted the reaction with **1** at 98 °C but this gave non-specific decomposition. The phosphine addition products **3** and **4** do not convert into the corresponding carbon–hydrogen and carbon–phosphorus bond activated products **5** and **6** upon further heating which suggests that these products are formed by different pathways. We propose that they share a common intermediate, namely the 50-electron clusters $[Ru_3(CO)_9\{P(C_4H_3E)_3\}\{\mu_3\text{-}\eta^1,\kappa^1,\kappa^2\text{-}PhP(C_6H_4)CH_2PPh\}]$ (**A**) (Scheme 5) and this is supported by previous work by Bonett and co-workers [9,10]. We are currently investigating the reactivity of **1** towards a range of mono- and bidentate phosphines in an attempt to find a high-yielding route to the metal-based formation of the dpbm ligand.

## Supplementary material

CCDC 729872, 729873 and 729871 contain the supplementary crystallographic data for this paper. These data can be obtained free of charge from The Cambridge Crystallographic Data Centre via www.ccdc.cam.ac.uk/data_request/cif.

## Acknowledgement

Financial support of this work by the University Grants Commission of Bangladesh is gratefully acknowledged.

## References

[1] (a) See for example, H. McFarlane, E. Christina, W. McFarlane, Polyhedron 18 (1999) 2117;
(b) F.B. McCormick, D.D. Cox, W.B. Gleason, Organometallics 12 (1993) 610;
(c) K. Mashima, N. Komura, T. Yamagata, K. Tani, M. Haga, Inorg. Chem. 36 (1997) 2908;
(d) S.J.A. Pope, G. Reid, Dalton Trans. (1999) 1615;
(e) L.-C. Song, J.-T. Liu, Q.-M. Hu, L.-H. Weng, Organometallics 19 (2000) 643;
(f) E. Szlyk, R. Kucharek, I. Szymanska, L. Pazderski, Polyhedron 22 (2003) 3389.
[2] (a) See for example, R.J. Puddpehatt, Chem. Soc. Rev. (1983) 99;
(b) B. Chaudret, B. Delavaux, R. Poilblanc, Coord. Chem. Rev. 86 (1988) 134;
(c) G.K. Anderson, Adv. Organomet. Chem. 35 (1993) 1.
[3] (a) See for example, R.B. Bedford, M. Huwe, M.C. Wilkinson, Chem. Commun. (2009) 600;
(b) M. Arisawa, T. Suzuki, T. Ishikawa, M. Yamaguchi, J. Am. Chem. Soc. 130 (2008) 12214;
(c) G. Hilt, W. Hess, K. Harms, Synthesis (2008) 75;
(d) M. Fabbian, N. Marsich, E. Farnetti, Inorg. Chim. Acta 357 (2004) 2881;
(e) D.A. Culkin, J.F. Hartwig, J. Am. Chem. Soc. 124 (2002) 9330;
(f) J. Ledford, C.S. Shultz, D.P. Gates, Organometallics 20 (2001) 5266.
[4] (a) See for example, S.J. Dossett, A. Gillon, A.G. Orpen, J.S. Fleming, P.G. Pringle, D.F. Wass, M.D. Jones, Chem. Commun. (2001) 699;
(b) N.A. Cooley, S.M. Green, D.F. Wass, K. Heslop, A.G. Orpen, P.G. Pringle, Organometallics 20 (2001) 4769;
(c) A. Carter, S.A. Cohen, N.A. Cooley, A. Murphy, J. Scutt, D.F. Wass, Chem. Commun. (2002) 858;
(d) J.N.L. Dennett, A.L. Gillon, K. Heslop, D.J. Hyett, J.S. Fleming, C.E. Lloyd-Jones, A.G. Orpen, P.G. Pringle, D.F. Wass, J.N. Scutt, R.H. Weatherhaed, Organometallics 26 (2004) 6077;
(e) T. Agapie, S.J. Schofer, J.A. Labinger, J.E. Bercaw, J. Am. Chem. Soc. 126 (2004) 1304;
(f) K. Blann, A. Bollmann, J.T. Dixon, F.M. Hess, E. Killian, H. Maumela, D.H. Morgan, A. Neveling, S. Otto, Chem. Commun. (2005) 620;

(g) M.J. Overett, K. Blann, A. Bollmann, J.T. Dixon, F. Hess, E. Killian, H. Maumela, D.H. Morgan, A. Neveling, S. Otto, Chem. Commun. (2005) 622;
(h) A. Bollmann, K. Blann, J.T. Dixon, F.M. Hess, E. Killian, H. Maumela, D.S. McGuiness, D.H. Morgan, A. Neveling, S. Otto, M. Overett, A.M.Z. Slawin, P. Wasserscheid, S. Kuhlmann, J. Am. Chem. Soc. 126 (2004) 14712;
(i) G. Hoge, H.-P. Wu, W.S. Kissel, D.A. Pflum, D.J. Greene, J. Bao, J. Am. Chem. Soc. 126 (2004) 5966;
(j) H.-P. Wu, G. Hoge, Org. Lett. 6 (2004) 3645;
(k) S.M. Hansen, F. Rominger, M. Metz, P. Hofmann, Chem. Eur. J. 5 (1999) 557;
(l) P. Hofmann, C. Meier, W. Hiller, M. Heckel, J. Riede, M.U. Schmidt, J. Organomet. Chem. 490 (1995) 51;
(m) J.V. Barkley, M. Ellis, S.J. Higgins, M.K. McCart, Organometallics 17 (1998) 1725;
(n) J.V. Barkley, J.C. Grimshaw, S.J. Higgins, P.B. Hoare, M.K. McCart, A.K. Smith, J. Chem. Soc., Dalton Trans. (1995) 2901.
[5] M.E. Cucciolito, V. De Felice, I. Orabona, A. Panunzi, F. Ruffo, Inorg. Chim. Acta 343 (2003) 209.
[6] V. De Felice, N. Fraldi, G. Roviello, F. Ruffo, A. Tuzi, J. Organomet. Chem. 692 (2007) 5211.
[7] F.G. Mann, A.J.H. Mercer, J. Chem. Soc., Perkin I (1972) 2548.
[8] N. Maigrot, C. Charrier, L. Ricard, F. Mathey, Bull. Soc. Chim. Fr. 134 (1997) 853.
[9] N. Lugan, J.-J. Bonnet, J.A. Ibers, J. Am. Chem. Soc. 107 (1985) 4484.
[10] N. Lugan, J.-J. Bonnet, J.A. Ibers, Organometallics 7 (1988) 1538.
[11] M.I. Bruce, B.K. Nicholson, M.L. Williams, Inorg. Synth. 26 (1990) 265.
[12] G. Hogarth, S.E. Kabir, Coord. Chem. Rev. 253 (2009) 1285.
[13] SMART and SAINT Software for CCD Diffractometers, Version 6.1, Madison, WI, 2000.
[14] G.M. Sheldrick, SHELXTL PLUS, Version 6.1, Bruker AXS, Madison, W1, 2000.
[15] A.A. Torabi, A.S. Humphreys, G.A. Koutsantonis, B.W. Skelton, A.H. White, J. Organomet. Chem. 655 (2002) 227.
[16] L. Viau, A.C. Willis, M.G. Humphrey, J. Organomet. Chem. 692 (2007) 2086.
[17] S.E. Kabir, Md.R. Hassan, D.T. Haworth, S.V. Lindeman, T.A. Siddiquee, D.W. Bennett, J. Organomet. Chem. 692 (2007) 3936.
[18] A.J. Deeming, S.N. Jaysuriya, A.J. Arce, Y.De. Sanctis, Organometallics 15 (1996) 786.
[19] M.A. Mottalib, S.E. Kabir, D.A. Tocher, A.J. Deeming, E. Nordlander, J. Organomet. Chem. 692 (2007) 5007.
[20] M.N. Uddin, N. Begum, M.R. Hassan, G. Hogarth, S.E. Kabir, M. A Miah, E. Nordlander, D.A. Tocher, Dalton Trans. (2008) 6219.
[21] Md.I. Hyder, S.E. Kabir, M.A. Miah, T.A. Siddique, G.M.G. Hossain, Polyhedron 24 (2005) 1471.
[22] (a) J.P. Collman, W.P. Roper, J. Am. Chem. Soc. 87 (1965) 4008;
(b) A.F. Hill, Angew. Chem., Int. Ed. Engl. 39 (2000) 130.
[23] C. Babij, L. Chen, I.O. Koshevoy, A.J. Poë, Dalton Trans. (2004) 833.
[24] P.E. Garrou, Chem. Rev. 85 (1985) 171.
[25] M.N. Uddin, M.A. Mottalib, N. Begum, S. Ghosh, A.K. Raha, D.T. Haworth, S.V. Lindeman, T.A. Siddiquee, D.W. Bennett, G. Hogarth, E. Nordlander, S.E. Kabir, Organometallics 28 (2009) 1514.
[26] S. Ghosh, M. Khatun, D.T. Haworth, S.V. Lindeman, T.A. Siddiquee, D.W. Bennett, G. Hogarth, E. Nordlander, S.E. Kabir, J. Organomet. Chem. 694 (2009) 2941.